Rate Constants for Intramolecular Electron-transfer Reactions of Ruthenium-modified Histidine Mutants of Cytochrome b_2†

Emma Lloyd,[a] Karen Chapman,[b] Stephen K. Chapman,[b] Zhi-Shen Jia,[a] Meng-Chay Lim,[a] Nicholas P. Tomkinson,[a] G. Arthur Salmon[c] and A. Geoffrey Sykes*,[a]

[a] *Department of Chemistry, University of Newcastle, Newcastle upon Tyne NE1 7RU, UK*

[b] *Department of Chemistry, University of Edinburgh, Edinburgh EH9 3JJ, UK*

[c] *Cookridge Radiation Research Centre, University of Leeds, Cookridge Hospital, Leeds LS16 6QB, UK*

The cytochrome b_2 core derived from flavocytochrome b_2 has been expressed in *Escherichia coli* and four mutants Lys-56→His, Lys-51→His, Asn-42→His and Pro-41→His have been generated by site-directed mutagenesis. Ruthenium modification of the first three mutants with $[Ru(NH_3)_5(H_2O)]^{2+}$ led to the formation of singly modified His-56[$Ru(NH_3)_5$], His-51[$Ru(NH_3)_5$] and His-42[$Ru(NH_3)_5$] derivatives in 30–45% yield. However no modification was observed with Pro41His. Moreover no evidence was obtained for the formation of His-19[$Ru(NH_3)_5$], where His-19 is the unco-ordinated histidine present in wild-type and mutant cytochrome b_2 forms. Characterisation of the singly modified products by inductively coupled plasma analyses indicates an Fe:Ru ratio of 1:1 for all three derivatives. The NMR spectra of the Ru-modified proteins reveal specific broadening by the paramagnetic Ru^{III} of the characteristically sharp $C^{\varepsilon}H$ and $C^{\delta}H$ resonances assigned to His-56, His-51 and His-42, while the $C^{\varepsilon}H$ resonance due to His-19 is unaffected. Whereas the titration of unmodified His-56, His-51, His-42 and His-41 residues by ^1H NMR spectroscopy gave pK_a 6.4, 6.2, 6.5 and 6.4 respectively, His-19 did not similarly titrate in the pH 4.8–10.0 range, which is attributed to hydrogen bonding to a nearby residue. Using pulse radiolysis to generate the methyl viologen radical, $MV^{\bullet+}$, the metastable iron(II)ruthenium(III) form of the protein was obtained. Rate constants for intramolecular electron transfer from Fe^{II} to Ru^{III} were determined; 3.5 (His-56), 2.8 (His-51) and 78 s^{-1} (His-42) at I = 0.100 M. Edge-to-edge distances, from the nearest point on one or other of the axial haem ligands to the nearest point on the imidazole ring, are 10.8 (His-56), 9.8 (His-51) and 8.5 Å (His-42), and the driving force is close to 145 mV. Using the Beratan–Onuchic approach the most favourable pathways for electron transfer have been identified. For His-42 a direct through-bond pathway *via* axial His-43 to the haem Fe is indicated. In the case of the His-56 and His-51 derivatives, pathways that include through-space interactions appear to be dominant.

Experiments on Ru-modified metalloproteins have shown that rate constants for intramolecular electron transfer are sensitive not only to the effects of distance and driving force, but also to protein structure.[1,2] Compared to studies by Dutton and colleagues,[3] studies on Ru-modified proteins with lower driving forces do not conform to a linear log k *vs.* distance relationship, and further understanding is required. Reactions which have been studied include Ru-modified plastocyanin,[4] azurin,[5] cytochrome c_{551},[6] cytochrome c peroxidase[7] and the high-potential iron–sulfur protein from *Chromatium vinosum*,[8] where discrepancies do not appear to be explained in terms of distance or driving force. Experimental approaches aimed specifically at examining the role of the intervening polypeptide medium are therefore required. The problem relates to the electronic coupling of redox centres through the protein. A significant contribution is the computational approach developed by Beratan and colleagues[9–12] in which a search for electron-transfer pathways which maximises the overall coupling is carried out. The model used assesses through-bond, hydrogen-bond and through-space routes and predicts which pathways are likely to be dominant. This approach appears to provide a better explanation of some kinetic data for Ru-modified proteins[1,2] than does the through-space distance approach.

We decided to use the cytochrome b_2 domain of flavocytochrome b_2 further to investigate such effects. A recent review on flavocytochrome b_2 (L-lactate; cytochrome c oxidoreductase, E.C. 1.1.2.3) has appeared.[13] The enzyme from baker's yeast (*Saccharomyces cerevisiae*) is a tetramer of identical subunits (M_r 57 500; 488 amino acids).[14] Each subunit consists of two distinct domains, a flavin mononucleotide domain (residues 101–511) and a haem-containing or cytochrome domain (residues 1–100). Complete amino-acid sequences are available for flavocytochrome from both baker's yeast,[15,16] and *H.anomala*,[17] and a crystal structure of 2.4 Å resolution has been determined for the *S.cerevisiae* enzyme.[18]

Under the action of a protease the haem domain (residues 8–103) of flavocytochrome b_2 can be released as a stable entity, and is referred to as cytochrome b_2 core.[19] A cleaner and higher-yield method of producing this protein has been achieved by expressing the core (residues 6–100) independently in *Escherichia coli*.[20] The proteins produced by proteolysis or by expression in *E.coli* have been shown to be essentially identical in terms of their physical properties.[20] The wild-type cytochrome b_2 core has axial ligands His-43 and His-66, and a single surface histidine at position 19. Four mutant forms of the core have been engineered by site-directed mutagenesis, Lys-56→His, Lys-51→His, Asn-42→His and Pro-41→His with histidines positioned at different distances and orientations to the porphyrin ring. The titration behaviour of these different histidines, monitored using NMR spectroscopy, has been investigated, since an understanding of the protonation/deprotonation properties can give an indication

† *Non-SI units employed:* M = mol dm^{-3}, eV ≈ 1.60 × 10^{-19} J.

Table 1 Ratios of Fe:Ru for the products of the reaction of cytochrome b_2 cores with $[Ru(NH_3)_5(H_2O)]^{2+}$

Core	Peak 1	Peak 2	Peak 3
Lys56His b_2	1:1.03	1:0.10	1:1.34
Lys51His b_2	1:0.99	1:0.05	1:1.63
Asn42His b_2	1:1.03	1:0.11	

as to the reactivity of different histidines towards $[Ru(NH_3)_5(H_2O)]^{2+}$.

Three Ru-modified derivatives of the cytochrome b_2 core mutants, His-56[$Ru(NH_3)_5$], His-51[$Ru(NH_3)_5$] and -42[$Ru(NH_3)_5$] have been prepared, and the intramolecular electron-transfer reactivity from Fe^{II} to Ru^{III} of each examined in order to investigate the effect of the intervening protein structure on electron-transfer rate constants.

Experimental

DNA Manipulation, Strains, Media and Growth.—*Escherichia coli* HB101 harbouring the vector pDS core (which is a modified form of pDS6)[20] was used for expression of the cytochrome b_2 haem domains as previously reported.[20] Mutagenesis was performed with single-stranded DNA from an M13mp 19 clone as previously described,[21] containing the haem domain coding sequence and using the following oligonucleotides: 172B (ATGCCGGGCATGATGTCAC), for Lys-56→His; 170B (ATGTTACCATTTTAATGCC), for Lys-51→His; and 171B (TCCTACCACATCATCCAG), for Asn-42→His. Resulting mutated clones were screened by hybridisation to the oligonucleotide used for mutagenesis. Positive mutants were verified by DNA sequencing and the *Eco*R1 fragments containing the haem domain coding sequences were inserted into the *Eco*R1 site of pDS6. Recombinants were selected with the correct orientation of the inserts for expression. Following subcloning, the inserts were sequenced in their entirety to verify the presence of the mutations and the absence of unwanted mutations in the coding sequences. Standard methods for growth of *E.coli*, plasmid purification, DNA manipulation and transformation were performed as described.[22]

Cell Growth.—Wild-type cytochrome b_2 core and all three mutants were grown and isolated in essentially the same manner. Cytochrome b_2 core which had been expressed in *E.coli* was grown from agar plates in a 50 l fermenter using a growth media of tryptone (10 g, Bacto), yeast extract (5 g, Bacto), and NaCl (5 g; BDH, Analar) per litre. Ampicillin (0.10 g l^{-1}) was added to the growth media. Cells were grown at 37 °C, and air was bubbled through the media throughout the growing at a rate of 15 l min^{-1}. Pink cells were isolated by centrifugation and stored at −80 °C until required.

Protein Isolation.—To isolate the protein from the pink cells, the paste was resuspended in 100 mM tris(hydroxymethyl)-aminomethane (Tris)–HCl pH 8.0 and lysozyme (≈0.2 mg cm^{-3}). The mixture was sonicated in 80 cm^3 portions using a Rapidis Soniprobe for 4 × 5 min, keeping the temperature < 10 °C by use of an ice–acetone bath. The sonicated mixture was centrifuged at 10 000 r.p.m. for 30 min (4 °C), and the supernatant was brought to 30% ammonium sulfate saturation. After stirring for 30 min the mixture was centrifuged again (10 000 r.p.m., 45 min), the pellet discarded, and the remaining solution brought to 70% ammonium sulfate saturation. The mixture was stirred for 1 h, and then the pink pellet containing the cytochrome was isolated by centrifugation at 10 000 r.p.m. (45 min). The pellet was redissolved in 5 mM Tris–HCl pH 8.0 (≈400 cm^3) and dialysed overnight against the same buffer at 4 °C. The dialysis buffer was changed twice at approximately 8 h intervals. The cytochrome sample was purified by anion-exchange chromatography (DE52, Whatman) using a linear gradient of 5–250 mM Tris–HCl pH 8.0. Further purification was achieved using a Sephadex G50-80 gel filtration column (Sigma), and fast protein liquid chromatography (FPLC) (Pharmacia) using a Mono Q column. Protein concentrations were determined from the absorbance of a haem chromophore at 413 nm (ε = 121.5 mM^{-1} cm^{-1}),[23] and protein purity was checked using the ratio of the absorbances at 413 and 280 nm. An absorbance ratio $A_{413}/A_{280} > 5.0:1$ is considered to indicate pure protein.

Ruthenium Complex.—All manipulations were carried out under a positive argon pressure. Pentaammineaquaruthenium(II) hexafluorophosphate was prepared from pentaammine-chlororuthenium(III) chloride, $[Ru(NH_3)_5Cl]Cl_2$, *via* conversion into the corresponding trifluoromethanesulfonate (triflate) complex, $[Ru(NH_3)_5(O_3SCF_3)][O_3SCF_3]_2$.[24] The method used to prepare the $[Ru(NH_3)_5(H_2O)][PF_6]_2$ complex was an adaptation of that of Curtis *et al.*[25] Dry zinc shot was freshly amalgamated with $HgCl_2$, and placed with the triflate salt (0.5 g) in an Ar-flushed flask. Deaerated water (5 cm^3) was added, weakly acidified with one drop of trifluoroacetic acid, when the complex dissolved immediately to give a dark blue solution which turned green then yellow after argon bubbling for ≈3 h. The solution was transferred by argon pressure to a stirred solution of ammonium hexafluorophosphate (3.75 g) in water (5 cm^3) causing immediate precipitation of a yellow solid. The precipitate was collected on an air-free sinter filtration apparatus and washed with Ar-flushed ethanol then diethyl ether.

Ruthenium Modification.—Essentially the same Ru-modification procedure was adapted for all three cytochrome b_2 core mutants. All manipulations were carried out under argon. Protein samples were purified by FPLC prior to the modification reaction and were then exchanged into Ar-flushed 20 mM *N'*-(2-hydroxyethyl)piperazine-*N*-ethane-2-sulfonic acid (hepes) pH 7.5 containing 0.10 M NaCl and concentrated to 3–4 cm^3. Pentaammineaquaruthenium(II) hexafluorophosphate was added in 50-fold excess to a second flask and dissolved in hepes buffer (3–5 cm^3). This was then transferred using an airtight syringe to the protein solution. Final protein concentrations were ≈2 mM. The reaction mixture was left in the dark under argon for the duration of the reaction times for the Lys56His, Lys51His and Asn42His cytochrome b_2 core mutants, *i.e.* 3.5, 4.25 and 4.0 h respectively. The reaction was terminated by loading the protein onto an air-free gel filtration column (G25-150 Sephadex, Sigma) and protein samples were immediately oxidised on elution from the column. The recovery was checked by measuring the absorbance at 413 nm and was usually in the range 85–90%. Reaction mixtures obtained from ruthenium modifications were purified by FPLC using Mono Q (anion-exchange) and Mono S (cation-exchange) columns (HR5/5, Pharmacia). Derivatives were obtained in 30–45% yields.

Reaction of mutant Lys56His cytochrome b_2 core with $[Ru(NH_3)_5(H_2O)]^{2+}$ yielded three major products. Two peaks, 1 and 2, were collected from the Mono Q column and an additional peak (3) was collected from the Mono S column. Peak 1 was of neutral charge and was eluted directly from both columns. Peaks 2 and 3 bound to the Mono Q and S columns, and eluted at ≈7% NaCl. The Fe:Ru ratios, obtained from inductively coupled plasma (ICP) atomic emission spectroscopy, are shown in Table 1. Peak 1 was assigned as a singly modified His-56[$Ru(NH_3)_5$] product on the basis of the Fe:Ru ratio of 1:1.03, and from the disappearance of the $C^{\varepsilon}H$ and $C^{\delta}H$ proton resonances of His-56 in the aromatic region of the ^1H NMR spectrum. Peaks 2 and 3 were assumed to be native (unmodified) Lys56His b_2 core and multiply modified Lys56His b_2 core and were not examined further.

The mutant Lys51His cytochrome b_2 core showed similar

behaviour and three major products were formed from the reaction with $[Ru(NH_3)_5(H_2O)]^{2+}$. Peak 1 eluted directly from the Mono Q column at ≈7% NaCl and peak 3 eluted from the Mono S column at ≈5% NaCl. The Fe:Ru ratios obtained from ICP analysis are shown in Table 1. Peak 1 showed specific broadening of the $C^{\varepsilon}H$ and $C^{\delta}H$ His-51 resonances in the ^1H NMR spectrum, and was assigned as singly modified His-51[$Ru(NH_3)_5$] b_2 core.

The reaction of mutant Asn42His with $[Ru(NH_3)_5(H_2O)]^{2+}$ yielded two major products with Fe:Ru ratios as shown in Table 1. Peak 1 was again of neutral charge and specific removal of the resonances attributed to the $C^{\varepsilon}H$ and $C^{\delta}H$ protons of His-42 was observed in the aromatic region of the spectrum. Peak 1 was therefore assigned as singly modified His-42[$Ru(NH_3)_5$] b_2 core.

Whereas the titration against H^+ of mutant Pro41His by NMR spectroscopy gives a pK_a of 6.4 for the His-41, which suggests that it should be modified by ruthenium, repeated attempts to do so were unsuccessful. It appears that Ru-modified Pro41His is very unstable and does not retain the ruthenium for a sufficient length of time for column purification to be carried out.

The singly modified His-56[$Ru(NH_3)_5$], His-51[$Ru(NH_3)_5$] and His-42[$Ru(NH_3)_5$] derivatives were also examined by NMR spectroscopy. Specific broadening of the resonances assigned to histidines 56, 51 and 42 in these derivatives, whilst the His-19 resonances remain unaffected, provides confirmation of ruthenium attachment at positions 56, 51 and 42 only.

Inductively Coupled Plasma Atomic Emission Spectroscopy (ICP-AES).—The Fe:Ru ratios for relevant fractions eluting from the FPLC were measured on a Bausch and Lomb ARL 3580 spectrometer at Johnson Matthey Technology Centre, Reading (Table 1). Sample concentrations (in ppm) were determined from the absorption at 413 nm, and were normally in the range 3–4 ppm Fe. Samples were frequently interspersed with internal standards to check for any drifts in the baseline on the ICP instrument. Three or four determinations were carried out for each sample to check reproducibility.

NMR Spectroscopy.—Proton NMR spectra were run at 25 °C on a Bruker 300 MHz NM300WB spectrometer in 10 mM potassium phosphate pH 7.0 made up in D_2O, $I \approx 0.1$ M. Presaturation techniques were used to suppress the water signal, and spectra were referenced against the residual water signal at δ 4.800. Samples were purified by FPLC immediately prior to NMR experiments, and exchanged into deuteriated buffer using a small Amicon cell (10 cm^3) fitted with a YM5 membrane. Protein concentrations were typically ≈1 mM (1–2 cm^3). For NMR titrations, the pH of the sample was adjusted directly in a NMR tube by additions of small aliquots (< 5 μl) of 0.10 M NaOD or DCl administered by means of a 50 μl Hamilton syringe. Measurements of pH were with a narrow CMAWL/3.7/180 combination electrode (Russell), and pH readings were not corrected for the deuterium isotope effect and correspond therefore to pH*. Spectra were discarded if the pH readings before and after the NMR experiment did not agree within 0.2 of a pH unit.

The titration behaviour of histidines 19, 56, 51, 42 and 41 in wild-type and mutant cytochrome b_2 cores was examined by NMR spectroscopy. The assignment of the His-19 $C^{\varepsilon}H$ proton resonance in wild-type cytochrome b_2 core was based on the ^1H NMR spectrum of cytochrome b_5 which has a sharp ^1H resonance at $\delta \approx 7.9$.[26,27] Assignment of the His-19, His-56, His-51, His-42 and His-41 $C^{\varepsilon}H$ resonances [imidazole ring atoms are γ, δ (× 2) and ε (× 2) respectively] in the mutant cytochromes was by comparison to the wild-type b_2 core spectrum and the spectrum of cytochrome b_5. The sharp singlet attributed to the $C^{\varepsilon}H$ resonance of His-19 in the wild-type and mutant cytochromes showed no changes in its chemical shift in the range pH 4.8–10.0. The $C^{\varepsilon}H$ resonances of His-56, His-51, His-42 and His-41 in the mutant Lys56His, Lys51His, Asn42His and Pro41His cytochromes however showed normal titration behaviour. The values of the chemical shift for the $C^{\varepsilon}H$ resonance for histidines 56, 51, 42 and 41 with variation in pH are listed in Table 2. From these data the pK_a values of 6.4, 6.2, 6.5 and 6.4 (all ±0.1) for histidines 56, 51, 42 and 41 respectively were fitted.

Pulse Radiolysis.—Experiments were carried out at Cookridge Radiation Research Centre, University of Leeds, using established procedures.[28] Experiments were carried out at 19 ± 1.5 °C and used 1 cm path-length cells. Radiation doses were adjusted so that the yield of reducing radical was ≤ ≈10% of the protein concentration. The yield of reducing radical for each pulse was calculated from the secondary-emission-chamber voltage reading which was calibrated prior to the experiment using thiocyanate dosimetry.[29]

The long-lived methyl viologen (1,1′-dimethyl-4,4′-bipyridinium dichloride) radical, $MV^{\bullet+}$ ($E^{\circ\prime} = -449$ mV)[30] was used as a reducing agent and its decay monitored at 605 nm. Absorption changes due to the iron(III)/iron(II) haem chromophore were monitored at 557 nm ($\Delta\varepsilon = 1.99 \times 10^4$ M^{-1} s^{-1}). Protein samples for pulse radiolysis were made up in 40 mM potassium phosphate pH 7.0 containing 0.012 M sodium formate, and 5×10^{-4} M methyl viologen (Sigma). Samples were bubbled with N_2O before pulsing. Under these conditions hydrated electrons are converted into $OH^{\bullet}$ radicals, and in the presence of formate all $OH^{\bullet}$ and $H^{\bullet}$ radicals are converted into $CO_2^{\bullet-}$, equation (1). Formate radicals react quantitatively with

Table 2 Variation in the position of the $C^{\varepsilon}H$ proton resonance of the histidine in four different cytochrome b_2 core mutants on pH titration. Spectra were run at 25 °C in 10 mM potassium phosphate buffer

(*a*) Mutant Lys-56→His

pH	8.60	8.20	7.60	7.30	6.75	6.41	6.25	5.92	5.65	4.65
δ	7.802	7.792	7.817	7.859	8.051	8.271	8.352	8.711	8.730	8.730

(*b*) Mutant Lys-51→His

pH	8.80	7.40	7.00	6.50	6.25	5.80	5.15	4.87
δ	7.785	7.836	7.895	8.057	8.308	8.422	8.618	8.659

(*c*) Mutant Asn-42→His

pH	8.75	7.30	6.77	6.30	6.00	5.50	5.60
δ	7.980	8.034	8.295	8.574	8.614	8.839	8.873

(*d*) Mutant Pro-41→His

pH	8.79	8.06	7.80	7.20	6.89	6.30	5.95	5.11	3.89
δ	7.966	7.988	8.000	8.140	8.145	8.534	8.691	8.889	8.937

$$HCO_2^- + OH^{\bullet}(H^{\bullet}) \longrightarrow CO_2^{\bullet -} + H_2O(H_2) \quad (1)$$

MV^{2+} to produce the $MV^{\bullet +}$ radical, equation (2). Signals

$$CO_2^{\bullet -} + MV^{2+} \longrightarrow MV^{\bullet +} + CO_2 \quad (2)$$

generated by pulse radiolysis were recorded on a Gould 4072 100 MHz Transient Digitiser and were transferred to a DEC 11/73 computer for storage and processing. Data were analysed using the program TREAT.[31] First-order rate constants were obtained by plotting $\ln[(A_\infty - A_t)/(A_\infty - A_0)]$ against time using a weighted linear least-squares procedure. Some traces were analysed using a program, FACSIMILE,[32] running on an Elonex 386S with coprocessor, 70 MByte hard disc and 4 MByte random access memory. Traces were transferred to the Elonex as EDI files using a file-transfer program KERMIT.

Results

Rate constants obtained for the reaction of unmodified cytochrome b_2 core mutants in the iron(III) state with the $MV^{\bullet +}$ radical are listed in Table 3. The stability of the iron(II) absorbance was also checked over long time-scales. No decay was observed over time-scales of as long as 100 ms per division. Rate constants for the reaction of $MV^{\bullet +}$ with Ru-modified iron(III)ruthenium(III) mutants were also determined at 557 nm, Table 4. From absorbance changes it was concluded that the reactions were partitioned between reduction at the iron(III) and ruthenium(III) centres, 63 and 37% for Lys56His, and 53 and 47% for both Lys51His and Asn42His, equations (3) and (4) respectively. Over longer time-scales a second stage was

$$Fe^{III}Ru^{III} + MV^{\bullet +} \longrightarrow Fe^{II}Ru^{III} \quad (3)$$

$$Fe^{III}Ru^{III} + MV^{\bullet +} \longrightarrow Fe^{III}Ru^{II} \quad (4)$$

observed, Fig. 1, in which the metastable $Fe^{II}Ru^{III}$ decays by intra- and inter-molecular processes, (5) and (6). The decay of

$$Fe^{II}Ru^{III} \xrightarrow{k_{intra}} Fe^{III}Ru^{II} \quad (5)$$

$$Fe^{II}Ru^{III} + Fe^{III}Ru^{III} \xrightarrow{k_{inter}} Fe^{III}Ru^{III} + Fe^{III}Ru^{II} \quad (6)$$

the iron(II) absorbance was monitored at 577 nm. The dependence of observed rate constants (Table 4) on the total concentration of oxidised protein is according to equation (7),

$$k_{obs} = k_{intra} + k_{inter}[Fe^{III}Ru^{III}] \quad (7)$$

where plots of k_{obs} against $[Fe^{III}Ru^{III}]$ give intercepts and slopes corresponding to the intra- and inter-molecular rate

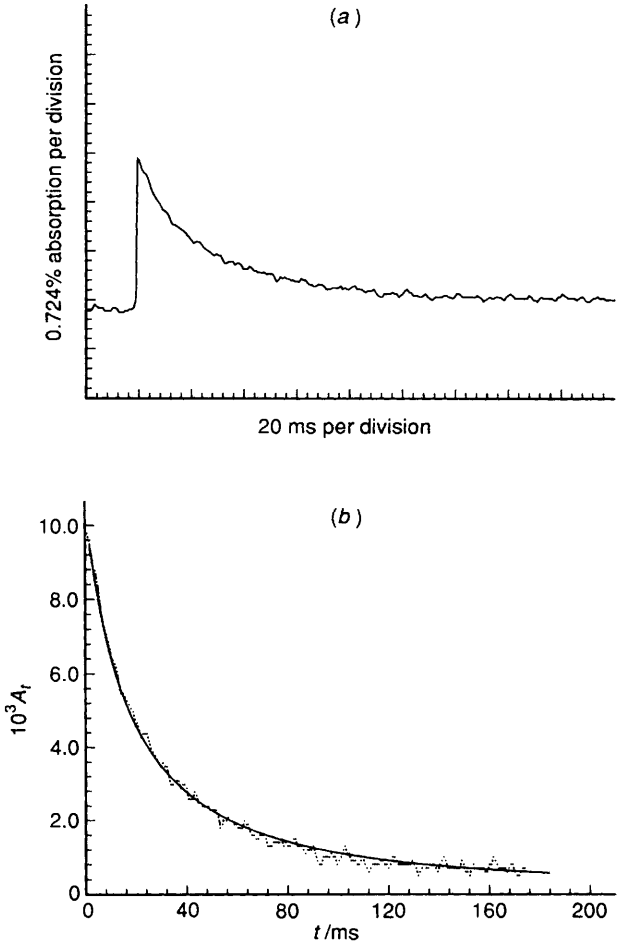

Fig. 1 Pulse radiolysis of (*a*) Ru-modified iron(III)ruthenium(III) Lys51His cytochrome b_2 core with methyl viologen radical, $MV^{\bullet +}$, showing the decay of the iron(II) absorbance at 557 nm, and (*b*) the corresponding kinetic fit obtained from the FACSIMILE fitting program.[32] Conditions: 19 °C, pH 7.0 (phosphate), I = 0.100 M. The variance of the fit in (*b*) is 0.275 (v = 218)

Table 3 Rate constants for the $MV^{\bullet +}$ reduction of fully oxidised iron(III)ruthenium(III) cytochrome b_2 core mutants in pulse-radiolysis experiments at 19 °C, pH 7.0 (0.10 M phosphate), I = 0.100 M. Errors are given in parentheses

	$10^{-9}\,k/M^{-1}\,s^{-1}$		
Mutant	Unmodified at 605 nm	Unmodified at 557 nm	Ru-modified at 557 nm
Lys56His	3.0 (0.03)	2.9 (0.10)	3.3 (0.10)
Lys51His	3.2 (0.10)	3.1 (0.10)	3.7 (0.10)
Asn42His	2.6 (0.04)	2.6 (0.04)	4.2 (0.03)

Table 4 First-order rate constants, k_{obs}, for the second stage of the reaction of $MV^{\bullet +}$ with Ru-modified iron(III)ruthenium(III) cytochrome b_2 cores corresponding to intra- and inter-molecular electron transfer from Fe^{II} to Ru^{III}. Experiments were carried out at 19 °C, pH 7.0, I = 0.100 M. Number of runs averaged in parentheses

(*a*) Lys56His mutant										
[Protein]/μM	2.5	2.5	4.0	4.0	5.8	5.8	7.4	9.0	9.0	12.0
k_{obs}/s^{-1}	8.5(2)	7.7	9.6	7.3	10.6(2)	11.1(2)	14.0(2)	14.8	17.2	21.5(2)
(*b*) Lys51His mutant										
[Protein]/μM	2.75	2.75	3.25	3.25	5.5	5.5	9.2	9.2	14.0	14.0
k_{obs}/s^{-1}	4.6(2)	4.5(2)	5.9	6.0	9.0	8.8	13.1(2)	16.2(2)	17.0	25.5(3)
(*c*) Asn42His mutant										
[Protein]/μM	2.4	2.4	4.7	4.7	6.5	6.5	6.5	6.5	10.3	10.3
k_{obs}/s^{-1}	95(2)	97	104	108(2)	125	129	123	121	151	150(2)

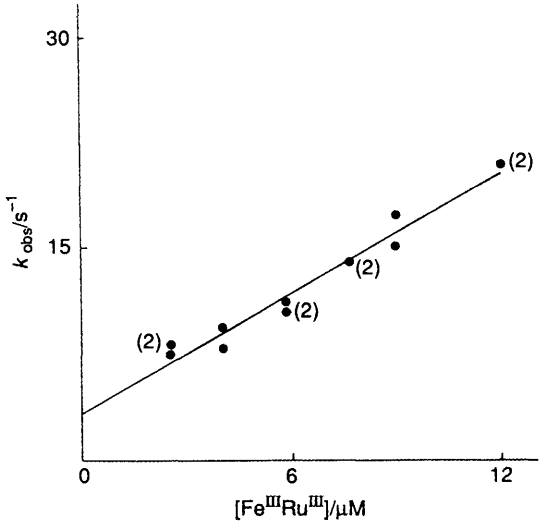

Fig. 2 The dependence of first-order rate constants, k_{obs} (19 °C), for the decay of the iron(II)ruthenium(III) form of the Lys56His core cytochrome b_2 mutant generated in pulse-radiolysis experiments with $MV^{\bullet+}$ as reductant on the (excess) concentration of oxidised iron(III)ruthenium(III) protein at pH 7.0 (phosphate), I = 0.100 M. Number of runs averaged indicated in parentheses

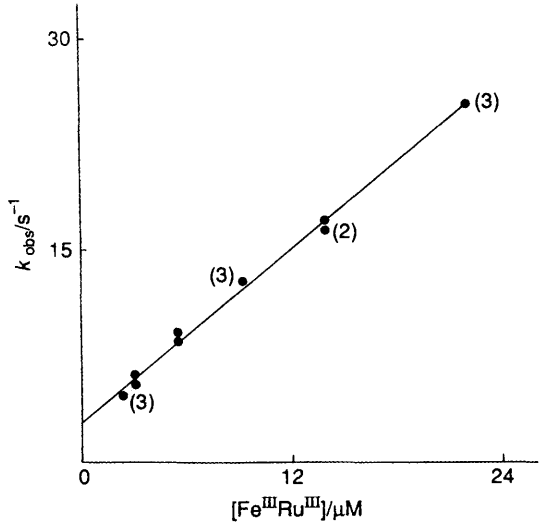

Fig. 3 The dependence of first-order rate constants, k_{obs} (19 °C), for the decay of the iron(II)ruthenium(III) form of the Lys51His core cytochrome b_2 mutant on the (excess) concentration of oxidised iron(III)ruthenium(III) protein. Other details as in Fig. 2

constants respectively, Figs. 2–4. Values of k_{intra} and k_{inter} are listed in Table 5. The kinetics showed evidence for small amounts of the second-order behaviour and the traces were therefore further analysed with the help of the computer program FACSIMILE.[32] Steps which might be considered are (8) and (9). Evidence for the presence of small amounts of Fe^{II}

$$Fe^{II}Ru^{III} + Fe^{II}Ru^{III} \longrightarrow Fe^{III}Ru^{II} + Fe^{III}Ru^{II} \quad (8)$$

$$Fe^{II}Ru^{III} + Fe^{II}Ru^{III} \longrightarrow Fe^{III}Ru^{III} + Fe^{II}Ru^{II} \quad (9)$$

was provided by the analysis of final absorbance readings.

Discussion

In this work four mutants of core cytochrome b_2 Lys56His, Lys51His, Asn42His and Pro41His, were prepared. These showed normal titration behaviour with pK_a values of 6.4, 6.2, 6.5 and 6.4. Single Ru-modified derivatives were obtained in three cases, His-56[$Ru(NH_3)_5$], His-51[$Ru(NH_3)_5$] and His-42[$Ru(NH_3)_5$], and were characterised by ICP and NMR spectroscopy. In the case of the fourth mutant, the loss of the structurally important Pro-41 residue close to the Fe (His-43 is one of the axial ligands) appears to be important, and using the same procedures no stable Ru-modified derivative was obtained.

We were also unable to modify the His-19 residue of wild-type cytochrome b_2, an observation that can be understood in terms of its pK_a. Assignment of the sharp ^1H NMR resonance of His-19 at $\delta \approx 7.9$ was made by comparison with the same His-19 in cytochrome b_5.[26,27] No shift in the C^eH resonance was observed in the range pH 4.8–10.0 in either the wild-type or mutant cytochrome b_2 cores indicating an anomalous pK_a. The crystal structures of both cytochrome b_2 and cytochrome b_5[33] provide important information regarding the environment of His-19. Thus the hydrogen of the N^δ is hydrogen bonded to the backbone carbonyl of Gln-11, and is believed to have a stabilising influence on one of the helices. Moreover the hydrogen bond is retained even in the absence of haem iron,[28] and the His-19 locality is implicated in the overall stability and rigidity of the molecule. Nor does the $N^\varepsilon H$ titrate,[34,35] and the pK_a is raised to an unusually high value. The corresponding titration on cytochrome b_5[36] gives a pK_a of 8.7 for His-19. In the case of cytochrome b_2 the pK_a of His-19 is even higher, since no shift is observed up to pH 10.0, and restrictions on His-19 are more extensive. The hydrogen bonding accounts for the lack of response of His-19 to ruthenium modification. Also relevant are our unsuccessful attempts to replace His-19 with asparagine or arginine using site-directed mutagenesis. The residue is structurally important,

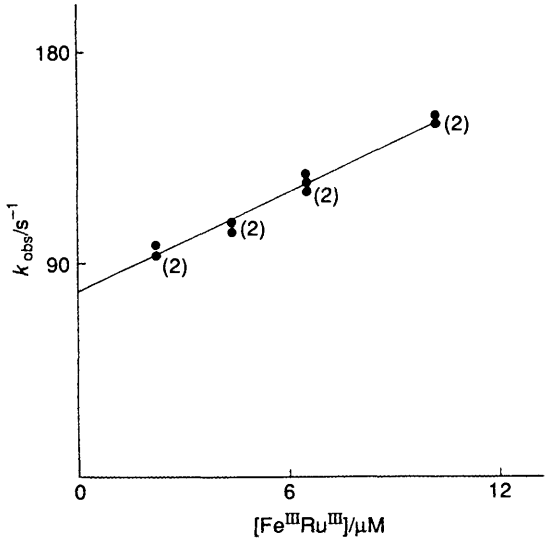

Fig. 4 The dependence of first-order constants, k_{obs} (19 °C), for the decay of the iron(II)ruthenium(III) form of the Asn42His core cytochrome b_2 mutant on the (excess) concentration of oxidised iron(III)ruthenium(III) protein. Other details as in Fig. 2

Table 5 Intra- and inter-molecular rate constant contributions to the decay of metastable iron(II)ruthenium(III) intermediates obtained in the pulse radiolysis of iron(III)ruthenium(III) cytochrome b_2 core mutants at 19 °C, pH 7.0 (0.10 M phosphate), I = 0.100 M. Errors are given in parentheses

Mutant	k_{intra}/s^{-1}	$10^{-6}\,k_{inter}/M^{-1}\,s^{-1}$
Lys56His	3.5 (0.7)	1.42 (0.11)
Lys51His	2.8 (0.2)	1.10 (0.02)
Asn42His	78 (2)	0.72 (0.02)

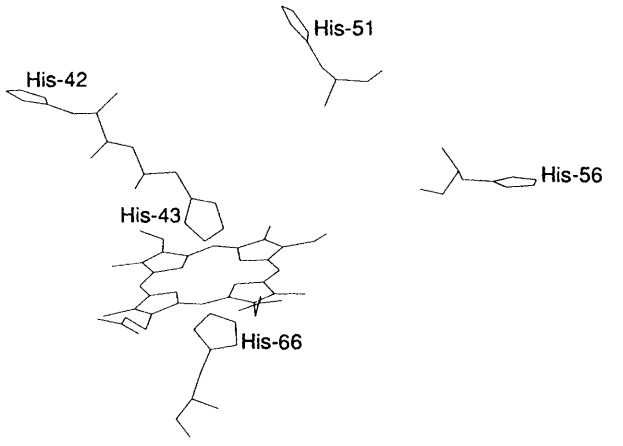

Fig. 5 The structure of cytochrome b_2 from molecular graphics indicating the positions of the imidazole rings of native His-66 and His-43 (both axially co-ordinated to the haem Fe), and His-56, His-51 and His-42 present in mutant forms. The latter were positioned by energy-minimisation procedures

as appears to be the case also with the invariant His-92 found in [2Fe-2S] ferredoxins, and this residue likewise is unreactive towards ruthenium modification as a result of its hydrogen-bonding interactions.[37]

Rate constants for the reaction of the methyl viologen radical $MV^{\bullet+}$ with unmodified Lys56His, Lys51His and Asn42His cytochrome b_2 cores, monitored at 605 and 557 nm, are in the range (2.6–3.2) × 10^9 M^{-1} s^{-1}, and no significant differences in behaviour are apparent. Similar kinetic behaviour is observed for the Ru-modified Lys56His, Lys51His and Asn42His cytochromes with rate constants for the reaction with $MV^{\bullet+}$ of 3.3 × 10^9, 3.7 × 10^9 and 4.2 × 10^9 M^{-1} s^{-1} respectively. In this case the reduction is divided between the haem iron(III) and the ruthenium(III) centres, equations (3) and (4). In contrast to the unmodified samples, where the iron(II) absorbances are stable over long time-scales, the three Ru-modified cytochromes showed a subsequent decay of the iron(II) absorbance. This type of behaviour can be accounted for in terms of contributions from intra- and inter-molecular electron-transfer processes, equations (5) and (6). A further kinetic feature was the observation that in all cases traces showed small deviations from first-order behaviour, and better fits to the experimental data were obtained using a scheme which incorporated additional equations (8) and (9).

The rate constants for Fe^{II} to Ru^{III} intramolecular electron transfer obtained from the three ruthenium-modified cytochromes His-56[$Ru(NH_3)_5$], His-51[$Ru(NH_3)_5$] and His-42[$Ru(NH_3)_5$] are 3.5, 2.4 and 78 s^{-1} respectively. The corresponding edge-to-edge distances from the nearest point on the axial haem ligand to the nearest point on the imidazole ring (*i.e.* the C^γ of the same residue in the native protein) are 10.8, 9.8 and 8.5 Å respectively. The positions of the histidine relative to the haem are indicated in Fig. 5. The driving force estimated from the reduction potentials of the Fe^{II}–Fe^{III} couple (−31 mV),[20] and the Ru^{II}–Ru^{III} couple (116 mV),[38] is close to 145 mV (0.14 eV).

Of singular importance in this work is the way in which the distance and the intervening polypeptide structure mediate the electron-transfer process. A recent advance is in the pathways program developed by Beratan and colleagues which searches for dominant electron-transfer routes through proteins and predicts the relative magnitude of the electronic coupling for each pathway. The program uses crystal-structure coordinates to search for combinations of covalent (C), hydrogen-bond (H) and through-space (S) interactions that maximise the tunnelling matrix element, T_{DA}, which for a single physical pathway can be written as in equation (10), where ε_i represents the decay of

$$T_{DA} = \text{prefactor} \prod_{i=1}^{N} \varepsilon_i \qquad (10)$$

the coupling for each particular type of interaction, C, H or S. An integral part of the theory is that each bond type contributes to the decay of the tunnelling matrix element in a predetermined manner; the decay factor for covalent bonds is mixed whilst for hydrogen-bond and through space interactions it decreases exponentially with distance.

Using the crystal-structure coordinates for flavocytochrome b_2,[18] the Beratan–Onuchic program has been implemented to examine the best electron-transfer pathways in the system. Since the study involves histidines at positions 56, 51 and 42, which are not present in the flavocytochrome b_2 structure, the pathway analysis has been carried out by taking the C^γ of Lys-56, Lys-51 and Asn-42 as the starting point for the electron-transfer pathway from the haem iron.

An important consideration is how much similarity exists between the mutant and the native structures. Although we have attempted to assess this using the crystal structure, some information is also available from NMR data. Thus NMR spectra of native and mutant proteins show essentially the same features, indicating that the tertiary structures in solution are similar. The question as to how similar the Ru-modified and native structures are is also raised? Again, in the absence of crystallographic evidence we are unable to address the point directly. A recent crystal structure for a Ru-modified cytochrome c peroxidase derivative[7] has indicated that the Ru-modified product is structurally similar to the native protein except for a rotation of the modified residue which is needed to accommodate the ruthenium complex. The present discussion rests on the assumption that the overall structural features are the same for the native, mutant and Ru-modified proteins. Similar assumptions have been made with other Ru-modified proteins,[39,40] and it has been noted[40,41] that the higher evolutionary variability of surface residues compared to buried residues seems to indicate that changing the identity of a residue at the surface is unlikely drastically to alter the overall protein structure.

For the His-56 mutant the pathway with the best electronic coupling ($\Pi_i\varepsilon_i$ = 2.67 × 10^{-4}) is a through-bond pathway from the N^δ of the haem His-66 ligand to the C^γ at position 56, incorporating the peptide backbone of Asp-57, Val-58 and Phe-62 (13C, 2H). An alternative possibility is available involving a through-space transfer of 4.15 Å from the C^α of the 2-vinyl group of the haem to the C^β of Val-58, followed by nine covalent linkages to the C^γ at position 56, with $\Pi_i\varepsilon_i$ = 2.05 × 10^{-4}. For the His-51 mutant a through-bond pathway, from the N^δ of His-43 through the peptide backbone atoms of Gly-46 and Gln-47 through to the C^γ at position 51, is again predicted to have the largest coupling value $\Pi_i\varepsilon_i$ = 3.18 × 10^{-3} (8C, 2H). Only one totally through-bond route is identified; all other routes include through-space transfers, the best employing a 3.05 Å jump from the C^α of the 2-vinyl group to the C^γ of Ile-50, followed by seven covalent transfers, $\Pi_i\varepsilon_i$ = 1.66 × 10^{-3}. For both the His-56 and His-51 mutants other through-space routes exist with coupling values close to the optimum value. Owing to the close proximity of the His-42 label to the axial His-43 ligand, through-bond pathways dominate for this mutant. The pathway with the best coupling has seven covalent transfers from the C^γ of His-43 to the C^γ at position 42, $\Pi_i\varepsilon_i$ = 2.80 × 10^{-2}, consistent with the Fe^{II} to Ru^{III} intramolecular rate constant of 78 s^{-1}. Although the pathway program is able to identify a rate enhancement for the His-42 derivative, it is not able satisfactorily to account for the apparent discrepancy between the rate constants for the His-56 and His-51 derivatives, 3.5 and 2.8 s^{-1} respectively, despite the shorter edge-to-edge distance and shorter through-bond pathway for the His-51 mutant.

Implicit in the analysis is the assumption that the reorganisation term, λ, is the same for all the mutants, so that the contribution of the Franck–Condon factor (FC) to the rate

constant in the Marcus equation is identical. For activationless electron transfer ($-\Delta G = \lambda$), FC is only weakly dependent on λ, equation (11).[42] Although large deviations in λ are not

$$FC = (4\pi\lambda kT)^{-\frac{1}{2}} \exp[-(\Delta G^\circ + \lambda)^2/4\lambda kT] \quad (11)$$

expected, when the driving force for electron transfer ($\approx$0.14 eV) is far from the activationless limit (a value of $\approx$1.2 eV has been implicated for Ru-modified cytochrome b_5[39]) spurious variations in λ are magnified since FC becomes exponentially dependent on λ, and a simple relationship between k for electron transfer and distance may no longer apply. This may help to account for the discrepancy between the His-56 and His-51 mutants.

Ruthenium modification of the His-41 mutant would have formed an interesting extension to this work as this mutant has a slightly longer through-bond pathway available, as well as through-space possibilities, and measurements of the intramolecular rate constant would have helped to identify whether through-bond (as in the His-42 mutant) or through-space (which appear to be important in the His-56 and His-51 mutants) interactions predominate. Repeated attempts to modify the His-41 mutant with ruthenium however did not allow this particular extension of the work to be completed.

Acknowledgements

We thank Johnson-Matthey plc and the SERC for a CASE Studentship (to E. L.), the Molecular Recognition Initiative of the SERC for providing molecular graphics facilities and post-doctoral funding (for N. P. T.), the Chinese Government for funding and Zhejiang Agricultural University for leave (to Z-.S. J.), and the University of Malaya for leave of absence (to M-.C. L.). We also thank Dr. Graeme Reid for helpful discussion.

References

1 D. N. Beratan, J. N. Onuchic and H. B. Gray, in *Metal Ions in Biological Systems*, eds. H. Sigel and A. Sigel, Marcel Dekker, New York, 1991, vol. 27, pp. 97–127; M. J. Therien, J. Chang, A. L. Raphael, B. E. Bowler and H. B. Gray, *Struct. Bonding (Berlin)*, 1991, **75**, 109; D. S. Wuttke, M. J. Bjerrum, J. R. Winkler and H. B. Gray, *Science*, 1992, **256**, 1007.
2 J. A. Bradley, M. R. Mauk, W. D. Funk, R. T. A. MacGillivray, A. G. Mauk and H. B. Gray, *J. Am. Chem. Soc.*, 1991, **113**, 4390; M. J. Therien, M. Selman and H. B. Gray, *J. Am. Chem. Soc.*, 1990, **112**, 2420.
3 C. C. Moser, J. M. Keske, K. Warncke, R. S. Farid and P. L. Dutton, *Nature (London)*, 1992, **355**, 796.
4 M.-P. Jackman, J. McGinnis, R. Powls, G. A. Salmon and A. G. Sykes, *J. Am. Chem. Soc.*, 1988, **110**, 5880.
5 R. Margalit, N. M. Kostic, C.-M. Che, D. F. Blair, H.-J. Chiang, I. Pecht, J. B. Shelton, J. R. Shelton, W. A. Schroeder and H. B. Gray, *Proc. Natl. Acad. Sci., USA*, 1984, **81**, 6554.
6 P. Osvath, G. A. Salmon and A. G. Sykes, *J. Am. Chem. Soc.*, 1988, **110**, 7114.
7 T. Fox, J. T. Hazzard, S.-L. Edwards, A. M. English, T. L. Poulos and G. Tollin, *J. Am. Chem. Soc.*, 1990, **112**, 7426.
8 M.-P. Jackman, M.-C. Lim, G. A. Salmon and A. G. Sykes, *J. Chem. Soc., Dalton Trans.*, 1988, 2843.
9 D. N. Beratan and J. N. Onuchic, *Photosynthesis Res.*, 1989, **22**, 173.
10 D. N. Beratan, J. N. Onuchic, J. N. Betts, B. E. Bowler and H. B. Gray, *J. Am. Chem. Soc.*, 1990, **112**, 7915.
11 D. N. Beratan, J. N. Onuchic and J. J. Hopfield, *J. Chem. Phys.*, 1987, **86**, 4488.
12 D. N. Beratan, J. N. Betts and J. N. Onuchic, *Science*, 1991, **252**, 1285.
13 S. K. Chapman, S. A. White and G. A. Reid, *Adv. Inorg. Chem.*, 1991, **36**, 257.
14 C. Jacq and F. Lederer, *Eur. J. Biochem.*, 1974, **41**, 311.
15 B. Guiard, *EMBO*, 1985, **4**, 3265.
16 F. Lederer, S. Cortial, A. M. Becam, P. Y. Hammont and L. Perez, *Eur. J. Biochem.*, 1985, **152**, 419.
17 M. T. Black, F. J. Gunn, S. K. Chapman and G. A. Reid, *Biochem. J.*, 1989, **263**, 973.
18 Z.-X. Xia and F. S. Matthews, *J. Mol. Biol.*, 1990, **212**, 837.
19 F. Labeyrie, O. Grovdinsky, Y. Jacquot-Armond and L. Naslin, *Biochim. Biophys. Acta*, 1966, **128**, 492.
20 C. E. Brunt, M. C. Cox, A. P. G. Thurgood, G. R. Moore, G. A. Reid and S. K. Chapman, *Biochem. J.*, 1992, **283**, 87.
21 G. A. Reid, S. A. White, M. T. Black, F. Lederer, F. S. Matthews and S. K. Chapman, *Eur. J. Biochem.*, 1988, **178**, 329.
22 T. Maniatis, E. F. Fritsch and J. Sambrook, *Molecular Cloning: A Laboratory Manual*, Cold Spring Harbor Laboratory Press, Cold Spring Harbor, 1982.
23 P. Pajot and O. Grovdinsky, *Eur. J. Biochem*, 1970, **12**, 158.
24 R. W. Callahan, G. M. Brown and T. J. Meyer, *Inorg. Chem.*, 1975, **14**, 1443.
25 J. C. Curtis, B. P. Sullivan and T. J. Meyer, *Inorg. Chem.*, 1983, **22**, 224.
26 J. Altman, J. J. Lipka, I. Kuntz and L. Waskell, *Biochemistry*, 1989, **28**, 7516.
27 C. D. Moore, O. N. Al-Musky and J. T. J. Leconte, *Biochemistry*, 1991, **30**, 8357.
28 G. V. Buxton, *Adv. Inorg. Bioinorg. Mech.*, 1984, **3**, 131, and refs therein.
29 E. M. Fielden, in *The Study of Fast Processes and Transient Species*, eds. J. H. Baxendale and F. Bun, Dordrecht, 1982, p. 58.
30 E. Steckhan and T. Kuwana, *Ber. Bunsenges. Phys. Chem.*, 1974, **78**, 253.
31 F. Wilkinson, The TREAT Program, Internal Report, Cookridge Radiation Research Centre, Leeds, 1988.
32 A. R. Curtiss and W. P. Sweetenham, *FACSIMILE (CHECKMAT) Users Manual*, UKAEA Document, AERE (R12805), Harwell, Didcot.
33 F. S. Matthews, M. Levines and P. Argos, *J. Mol. Biol.*, 1972, **64**, 449.
34 W. F. Reynolds, I. R. Peat, M. H. Freedman and J. R. Lyerton, jun., *J. Am. Chem. Soc.*, 1973, **95**, 328.
35 M. Tanobura, *Biochem. Biophys. Acta*, 1983, **742**, 576.
36 R. E. Wasyholen and G. A. Tomkinson, *Can. J. Biochem.*, 1977, **55**, 579.
37 E. Lloyd, N. P. Tomkinson, G. A. Salmon and A. G. Sykes, *Biochim. Biophys. Acta*, 1993, **1202**, 113.
38 F. A. Armstrong, J. N. Betts, K. Govindaraju, J. McGinnis, R. Powls and A. G. Sykes, *Inorg. Chem.*, 1990, **29**, 4862.
39 B. A. Jacobs, M. R. Mauk, D. W. Funk, R. T. MacGillivray, A. G. Mauk and H. B. Gray, *J. Am. Chem. Soc.*, 1991, **113**, 4390.
40 B. E. Bowler, T. J. Meade, S. L. Mayo, J. H. Richards and H. B. Gray, *J. Am. Chem. Soc.*, 1989, **111**, 8757.
41 M. Go and S. Miyazawa, *J. Pept. Protein Res.*, 1980, **15**, 211.
42 P. Siddarth and R. A. Marcus, *J. Phys. Chem.*, 1993, **97**, 2400.

Received 10*th June* 1993; *Paper* 3/03348A